Dalton Transactions

COMMUNICATION

View Article Online
View Journal | View Issue

Cite this: *Dalton Trans.*, 2016, **45**, 5425

Received 14th January 2016,
Accepted 26th February 2016

DOI: 10.1039/c6dt00180g

www.rsc.org/dalton

Understanding the complexation of Eu^{3+} with three diglycolamide-functionalized calix[4]arenes: spectroscopic and DFT studies†

Seraj Ahmad Ansari,[a] Prasanta Kumar Mohapatra,*[a] Sheikh Musharaf Ali,[b] Arijit Sengupta,[a] Arunasis Bhattacharyya[a] and Willem Verboom[c]

Complexation of Eu^{3+} with three diglycolamide-functionalized calix[4]-arene (C4DGA) ligands was investigated by UV-Vis and luminescence spectroscopy measurements in acetonitrile medium. The complexation thermodynamics was studied by micro-calorimetry while structural information was obtained from DFT calculations.

Introduction

In view of high efficiency of diglycolamides (DGA)[1] as a class of organic ligands for the selective extraction of trivalent actinides and lanthanides from high level radioactive wastes as one of the most acceptable strategies of radioactive waste remediation, attempts have been made to synthesize multiple DGA-functionalized ligands and study their complexation/extraction properties.[2] Calix[4]arenes with DGA-functionalization in the narrow rim were evaluated for actinide ion extraction with very promising results.[3] Out of those, the calix[4]arenes with four DGA pendant arms (C4DGA) were found to be highly promising for actinide ion extraction and displayed unusual selectivities as compared to the ligands containing two DGA pendant arms (C2DGA).[4] There had been an attempt by us to understand the complexation behaviour of these ligands earlier.[4] This prompted us to study the actinide ion extraction using DGA-functionalized calix[4]arenes appended on to the narrow-rim, wide-rim and both sides of the scaffold (Fig. 1). While comparing the extraction behaviour of a C4DGA ligand functionalized on the narrow-rim ($\mathbf{L_I}$) *vis-à-vis* the wide-rim functionalized C4DGA ligand ($\mathbf{L_{II}}$), it was noticed that $\mathbf{L_I}$ was far more superior than $\mathbf{L_{II}}$.[3] However, our subsequent studies with a both sides functionalized calix[4]arene with eight DGA moieties (C8DGA, $\mathbf{L_{III}}$) though found not to be a very efficient extractant in molecular diluents,[3] showed significantly high distribution coefficient values for Am^{3+} ion extraction which almost remained unchanged over a wide range of HNO_3 concentration in a room temperature ionic liquid.[5] This warranted a thorough investigation of the comparative complexation of trivalent actinide/lanthanide ions with the three calix[4]arene ligands. Complexation studies carried out in the present work involved UV-vis and luminescence spectroscopy, and while thermodynamic parameters were obtained by micro-calorimetry, the complexed species were identified by the ESI-MS technique. Structural information was obtained from DFT calculations since attempts to obtain single crystals were not successful.[6] Furthermore, while previous studies with C4DGA and C2DGA ignored the complexation by nitrate ions, which are known to play an important role in metal ion extraction/complexation by the calix[4]arenes, we thought that it would be interesting to carry out DFT calculations on the metal ion complexation taking into consideration the presence of nitrate ions in the complexing medium. A Eu^{3+} (as a surrogate of Am^{3+}) ion was used for the complexation studies. To the best of our knowledge, this is the first ever report on the comparative complexation behaviour of three DGA-functionalized calix[4]arene ligands, $\mathbf{L_I}$, $\mathbf{L_{II}}$, and $\mathbf{L_{III}}$ with different modes of functionalization.

Results and discussion

Stability constants of Eu^{3+}/L complexes

All the three ligands ($\mathbf{L_I}$, $\mathbf{L_{II}}$, and $\mathbf{L_{III}}$) show strong absorption bands between 195 and 240 nm (Fig. S1†). Fig. 2 (left) shows representative spectrophotometric titrations of $\mathbf{L_I}$, $\mathbf{L_{II}}$, and $\mathbf{L_{III}}$ with Eu^{3+} in acetonitrile. Factor analysis of the spectra for all three titrations suggested that there were two absorbing species, the free ligand and the ML complex. The best fit was achieved by using the model which considered the formation of a 1 : 1 complex. The calculated molar absorptivities of the free ligands and the Eu^{3+}/L complexes are shown at the right

[a]*Radiochemistry Division, Bhabha Atomic Research Centre, Trombay, Mumbai-400085, India. E-mail: mpatra@barc.gov.in*
[b]*Chemical Engineering Division, Bhabha Atomic Research Centre, Trombay, Mumbai-400085, India*
[c]*Laboratory of Molecular Nanofabrication, MESA+ Institute for Nanotechnology, University of Twente, P.O. Box 217, 7500 AE Enschede, The Netherlands*
† Electronic supplementary information (ESI) available: Synthetic procedures, characterization details, analytical and extraction data. See DOI: 10.1039/c6dt00180g

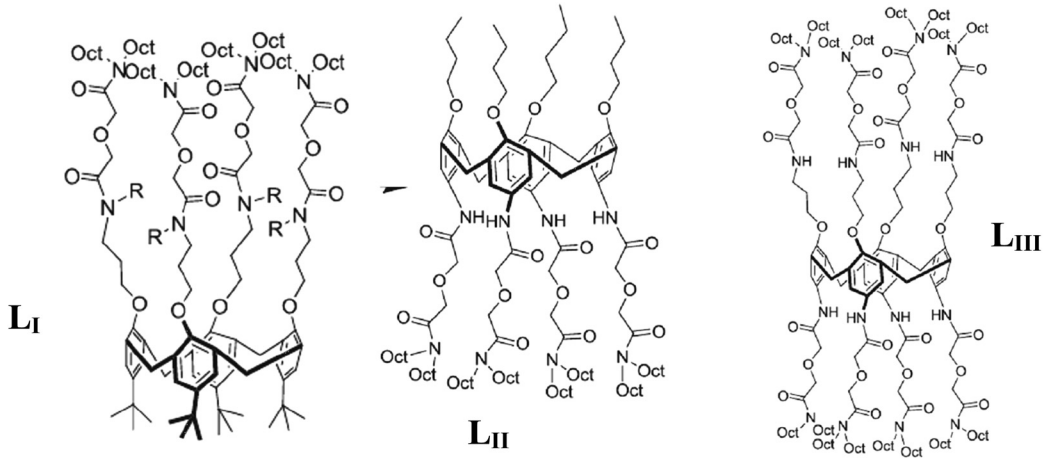

Fig. 1 Structural formulae of ligands.

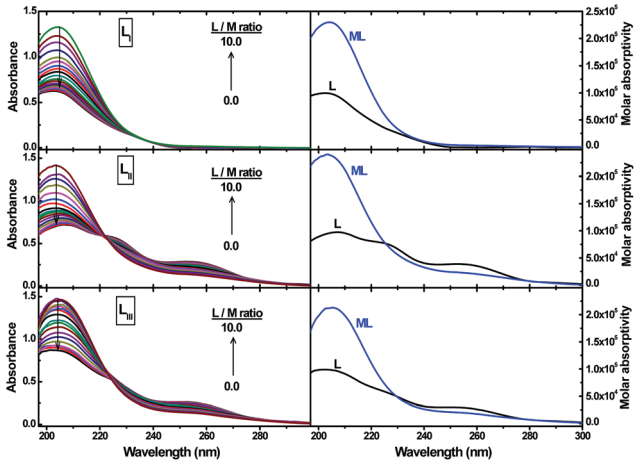

Fig. 2 Spectrophotometric titration of L_I, L_{II}, and L_{III} with Eu^{3+} in acetonitrile (left) and deconvoluted spectra of the absorbing species (right). Cuvette solution (2 mL): 0.005 mmol L^{-1} L_I, 0.008 mmol L^{-1} L_{II} or 0.006 mmol L^{-1} L_{III}; titrant: 0.10 mmol L^{-1} $Eu(NO_3)_3$; temperature: 25 °C.

Table 1 Thermodynamic data for the complexation of the ligands with Eu^{3+} in acetonitrile

Ligand	Log β	ΔH (kJ mol^{-1})	ΔS (J mol^{-1} K^{-1})
$\mathbf{L_I}$	7.35 ± 0.03	−22.5 ± 0.8	65 ± 3
$\mathbf{L_{II}}$	1.10 ± 0.02	−13.7 ± 0.4	−25 ± 2
$\mathbf{L_{III}}$	6.71 ± 0.02	−20.2 ± 0.7	61 ± 3

side of Fig. 2. The log β values of the three ligands with Eu^{3+} were calculated using non-linear least squares regression analysis[7] and the data are included in Table 1 following the order: $\mathbf{L_I} > \mathbf{L_{III}} \gg \mathbf{L_{II}}$ which is in line with what was seen in the solvent extraction studies of Am(III).[8] ^{13}C NMR spectral analysis of $\mathbf{L_I}$ and its La(III)–triflate complex (Fig. S1†) clearly showed a shift of the carbonyl peak indicating complex formation. In the case of $\mathbf{L_I}$, the four DGA moieties are attached to the calix[4]arene platform through the phenolic oxygens *via* a three-carbon atom spacer. The four-atom spacer between the DGA and the rigid calix[4]arene platform provides a better flexibility of the coordination sites, which eventually helps in a better coordination with the metal ions.[9] In contrast, the DGA groups are directly attached to the calix[4]arene platform in $\mathbf{L_{II}}$, resulting in a poor flexibility of the pendant arms to induce a favorable orientation of their coordination sites which explains the significantly lower log β value with $\mathbf{L_{II}}$. On the other hand, the stability constant with $\mathbf{L_{III}}$ is an order of magnitude lower than that of $\mathbf{L_I}$, but much larger than that of $\mathbf{L_{II}}$. If one assumes that both arms, upper and lower, in $\mathbf{L_{III}}$ are participating in the complexation, then one must end-up with a Eu^{3+}/L stoichiometry of 2 : 1. However, the best fit of the spectrophotometric titration data (Fig. 2) could be obtained only by assuming a 1 : 1 species. This observation confirms that only one side of the pendant arm is actually participating in the complexation. Since the thermodynamic data (Table 1) obtained by microcalorimetric titrations (Fig. S2, ESI†) of $\mathbf{L_{III}}$ are closer to that of $\mathbf{L_I}$, one may assume the participation of the narrow rim pendant arms in the complexation. The presence of the upper arms may bring more steric hindrance during the complexation, and therefore, the stability constant with $\mathbf{L_{III}}$ is lower than that of $\mathbf{L_I}$, though the same number of pendant arms are coordinating in both the cases. These arguments are supported by the thermodynamic data presented in Table 1, where the stability constant, enthalpy and entropy values with $\mathbf{L_I}$ and $\mathbf{L_{III}}$ are close to one another. Low exothermic enthalpy and negative entropy changes in the case of $\mathbf{L_I}$ is an indication of a poor stereochemical conformation of the complex, which eventually gives poor complexation with Eu^{3+}. We also tried to identify the Eu^{3+}/L complexes by ESI-MS, and the formation of a 1 : 1 metal/ligand complex was confirmed with all the three ligands (Fig. S3†).

Luminescence studies on Eu^{3+} complexes

Fig. 3(a) shows representative luminescence spectra of Eu^{3+} in the presence of $\mathbf{L_I}$ in acetonitrile. In particular, the intensity of

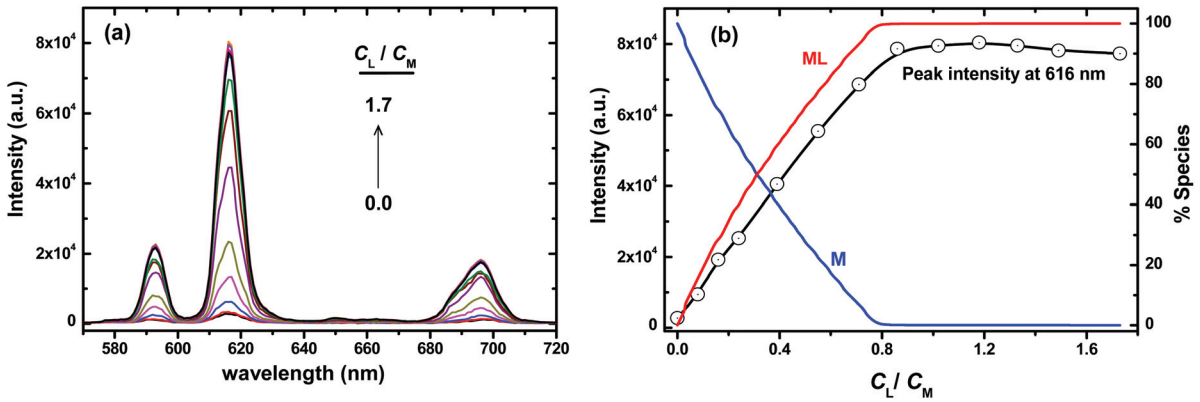

Fig. 3 Luminescence titration of $Eu(NO_3)_3$ with L_I. (a) Emission spectra; (b) intensity of the emission band at 616 nm (left side, *y*-axis) and the speciation of Eu^{3+} as a function of C_L/C_{Eu} (right side, *y*-axis). Excitation wavelength: 395 ± 5 nm; cuvette solution: 1.0 mmol L^{-1} $Eu(NO_3)_3$ (2.0 mL); titrant: 1.57 mmol L^{-1} L_I; temperature: 25 °C.

the hypersensitive $^5D_0 \rightarrow {}^7F_2$ transition (around 610–620 nm) increased significantly with increased ligand concentration from $C_L/C_{Eu} = 0$ to $C_L/C_{Eu} = 2$, indicating changes in the coordination environment around the central Eu^{3+} ion.[10] A plot of the peak intensity at 616 nm as a function of C_L/C_{Eu} (Fig. 3b) shows a gradual increase in the peak intensity up to a C_L/C_{Eu} ratio of 0.9, and remained constant thereafter, indicating the completion of the complexation reaction. This behavior is in line with the formation of $Eu(L)^{3+}$ species that was almost 100% complete at this ratio of C_L/C_{Eu}, as evident from the speciation diagram in Fig. 3b. A Job's plot by following the 616 nm emission peak intensity ($^5D_0 \rightarrow {}^7F_2$ transition) also pointed to the formation of a 1 : 1 metal/ligand species (Fig. S4†). Fluorescence lifetime measurements on the complex gave vital information about the number of water molecules in the primary coordination sphere of the Eu^{3+} ions (see Fig. S5†) and suggested almost no water molecules in the inner coordination sphere (Table S1†)[11] which suggested coordination of the metal ion by three pendant arms of the $\mathbf{L_I}$ acting as tridentates (ESI†). The mono-exponential nature of the ligand as shown in Fig. S5† also suggested a single complex species. Very recently, EXAFS measurements on Eu^{3+} with DGA ligands have confirmed the tridentate nature of the ligand in a 1 : 3 Eu^{3+}/DGA complex.[12] X-ray diffraction studies on a single crystal of the Am^{3+}/DGA complex confirmed that Am^{3+} is coordinated by nine oxygen atoms from three DGA ligands.[11]

DFT calculations

The minimum energy structures of the $Eu^{3+}/\mathbf{L_I}$ and $Eu^{3+}/\mathbf{L_{II}}$ complexes obtained from DFT calculations using TURBOMOLE[13] are depicted in Fig. 4(a) and (b), respectively. The calculated structural parameters for both the complexes, $\mathbf{L_I}$ and $\mathbf{L_{II}}$, are summarized in Table S2.† The Eu–O bond lengths for both the amide as well as the ether oxygen atoms in $Eu^{3+}/\mathbf{L_{II}}$ are longer than those in the $Eu^{3+}/\mathbf{L_I}$ complex. This suggests a stronger complex formation of Eu^{3+} with $\mathbf{L_I}$ as compared to that with $\mathbf{L_{II}}$. Furthermore, the metal oxygen bond distance with the amide oxygen is shorter than that with the ether oxygen, indicating a stronger interaction with the former. Our results are in conformity with the EXAFS results obtained on the Er^{3+}/DGA complex.[14]

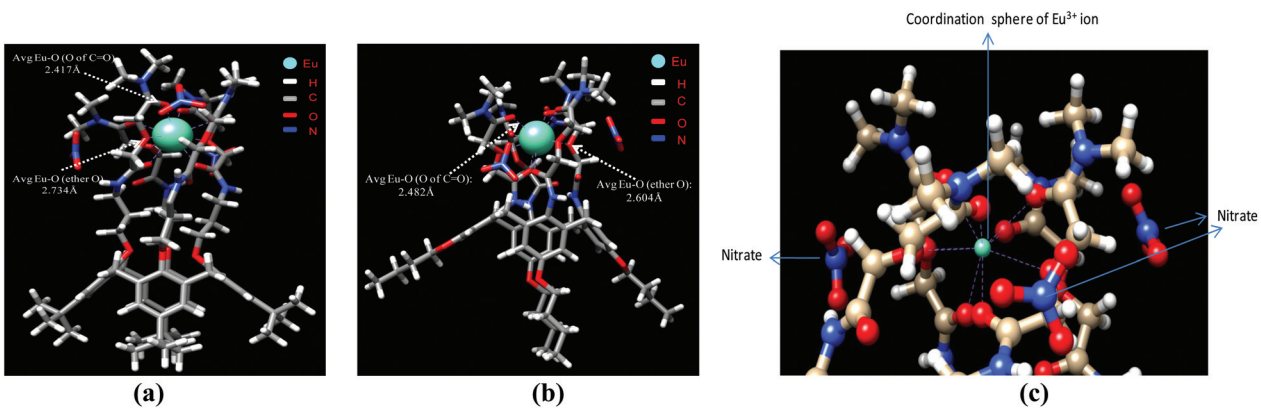

Fig. 4 Optimized structure of Eu^{3+}/nitrate complexes with L_I (a) and L_{II} (b) at the B3LYP/SVP level of theory. (c) Amplified view of coordinating sphere of Eu^{3+} ion with L_I and nitrate ions (L_I).

The free energy values for the complexation of Eu^{3+} ions with the ligands $\mathbf{L_I}$ and $\mathbf{L_{II}}$ in both the gas and the acetonitrile phase are presented in Table S3.† The explicit hydration of Eu^{3+} ions with nine water molecules in the first solvation shell was considered to evaluate the complexation free energy as it corresponds with the experimental solvation energy quite accurately.[15] The entropy of complexation was found to be positive and quite high. The well known COSMO solvation approach was used to simulate the solvent phase as it is able to predict the solvent phase properties quite accurately. The calculated solution phase free energies for the complexation are given in Table S3.† The free energy present in the gas phase is reduced considerably in the solution phase due to the dielectric screening of the acetonitrile. Both the gas phase as well as the solvent phase free energies of complexation with $\mathbf{L_I}$ are higher than with $\mathbf{L_{II}}$. This observation evokes that $\mathbf{L_I}$ forms a stronger complex with Eu^{3+} than $\mathbf{L_{II}}$, a fact also found experimentally. It is worth mentioning that a DFT calculation for the $Eu^{3+}/\mathbf{L_I}$ complex was performed previously though with an aim to compare with C2DGA ligands (with 2 DGA pendant arms).[4] The complexation energy was found to be −30.63 eV, lower than the energy calculated in the present work (−21.51 eV) which is attributed to the consideration of nitrate ions in the present work, which was not considered in the previous calculation.

In order to gain insight into the nature of the bonding in the Eu^{3+}/L complexes, the charge on the metal ions and the atomic orbital population in the complexes were analyzed using the natural population analysis (NPA) method.[16] The calculated values are given in Table S4.† The substantial positive charge on the Eu^{3+} ion indicates anion-dipole type of interaction in both cases, $\mathbf{L_I}$ and $\mathbf{L_{II}}$. The interaction sites of the donor can be easily visualized from the molecular electrostatic potential as given in Fig. 4(c).

The $E_{HOMO-LUMO}$ of the Eu^{3+} ion (3.64 eV, Table S5†) is very close to that of $\mathbf{L_I}$ (3.74 eV) resulting in a higher interaction energy than in the case of $\mathbf{L_{II}}$, having an $E_{HOMO-LUMO}$ value of 4.77 eV. The calculated values of the absolute hardness, η, and the absolute electronegativity, χ, are higher for $\mathbf{L_{II}}$ than for $\mathbf{L_I}$. The binding energy trend cannot be correlated with the values of η and χ. The amount of charge transfer, ΔN, was also calculated for the donor acceptor interaction and the values are presented in Table S5.† The higher the value of charge transfer, ΔN, the higher is the metal–ligand interaction. In the present case, the value of ΔN is higher with $\mathbf{L_I}$ than with $\mathbf{L_{II}}$ and hence shows a higher binding energy in the case of $\mathbf{L_I}$.

Conclusions

The complexation of Eu^{3+} ions with the three diglycolamide functionalized calix[4]arene ligands, $\mathbf{L_I}$, $\mathbf{L_{II}}$, and $\mathbf{L_{III}}$, suggested a stronger complex formation with $\mathbf{L_I}$ as compared to the remaining two ligands due to a favorable pre-orientation of the coordinating sites. All three ligands form 1 : 1 ML complexes (M = Eu^{3+}, and L = ligand) without any inner-sphere water molecules and the species could be confirmed by ESI-MS. The structural studies on the complexes indicate the participation of three diglycolamide pendant arms in the binding *via* two carbonyl oxygen and one ether oxygen atom. The gas as well as the solvent phase free energy of Eu^{3+}/L complexation, calculated using hybrid DFT, confirm the higher interaction of $\mathbf{L_I}$ with Eu^{3+} compared to $\mathbf{L_{II}}$. Bonding analysis by DFT indicated the electrostatic and slightly covalent nature of the interactions between the metal ions and the chelating ligands. The strong complexation of the trivalent lanthanide ion can be extrapolated to the trivalent minor actinide ions such as Am^{3+} and Cm^{3+} and can be exploited for their separation from radioactive wastes containing a host of other radionuclides.

SAA, PKM, AS and AB thank Dr P. K. Pujari, Head Radiochemistry Division, for his keen interest in this work.

Notes and references

1 S. A. Ansari, P. N. Pathak, P. K. Mohapatra and V. K. Manchanda, *Chem. Rev.*, 2012, **112**, 1751–1772.
2 (*a*) D. Jańczewski, D. N. Reinhoudt, W. Verboom, C. Hill, C. Allignol and M. T. Duchesne, *New J. Chem.*, 2008, **32**, 490–495; (*b*) A. Leoncini, P. K. Mohapatra, A. Bhattacharyya, D. R. Raut, A. Sengupta, P. K. Verma, N. Tiwari, D. Bhattacharyya, S. Jha, A. M. Wouda, J. Huskens and W. Verboom, *Dalton Trans.*, 2016, **45**, 2476–2484.
3 M. Iqbal, P. K. Mohapatra, S. A. Ansari, J. Huskens and W. Verboom, *Tetrahedron*, 2012, **68**, 7840–7847.
4 D. R. Raut, P. K. Mohapatra, S. A. Ansari, S. V. Godbole, M. Iqbal, D. Manna, T. K. Ghanty, J. Huskens and W. Verboom, *RSC Adv.*, 2013, **3**, 9296–9303.
5 P. K. Mohapatra, A. Sengupta, M. Iqbal, J. Huskens, S. V. Godbole and W. Verboom, *Dalton Trans.*, 2013, **42**, 8558–8562.
6 Several attempts to grow single crystals were unsuccessful and yielded pastes.
7 P. Gans, A. Sabatini and A. Vacca, *Talanta*, 1996, **43**, 1739–1753.
8 P. K. Mohapatra, D. R. Raut, M. Iqbal, J. Huskens and W. Verboom, *J. Membr. Sci.*, 2013, **444**, 268–275.
9 P. K. Mohapatra, A. Sengupta, M. Iqbal, J. Huskens and W. Verboom, *Inorg. Chem.*, 2013, **52**, 2533–2541.
10 P. Zhang and T. Kimura, *Solvent Extr. Ion Exch.*, 2006, **24**, 149–163.
11 P. P. Barthelemy and G. R. Choppin, *Inorg. Chem.*, 1989, **28**, 3354–3357.
12 M. R. Antonio, D. R. McAlister and E. P. Horwitz, *Dalton Trans.*, 2015, **44**, 515–521.
13 (*a*) R. Ahlrichs, M. Bar, M. Haser, H. Horn and C. Kolmel, *Chem. Phys. Lett.*, 1989, **162**, 165–169; (*b*) TURBOMOLE V6.0 2009, a development of the University of Karlsruhe and Forschungszentrum Karlsruhe GmbH, TURBOMOLE GmbH, 1989–2007.

14 H. Narita, T. Yaita and S. Tachimori, *Proceeding of ISEC*, *Soc. Chem. Ind.*, 1999, pp. 693–696.
15 A. K. Singha Deb, S. M. Ali, K. T. Shenoy and S. K. Ghosh, *Mol. Simul.*, 2015, **41**, 490–503.
16 (*a*) A. E. Reed and F. Weinhold, *J. Chem. Phys.*, 1983, **78**, 4066–4073; (*b*) A. E. Reed and F. Weinhold, *J. Chem. Phys.*, 1985, **83**, 735–746; (*c*) A. E. Reed, L. A. Curtiss and F. Weinhold, *Chem. Rev.*, 1988, **88**, 899–926.